Journal of Ceramic Processing Research. Vol. 12, No. 5, pp. 504~508 (2011)

J O U R N A L O F
Ceramic Processing Research

Effect of calcination temperature on the particle sizes of zinc ferrite prepared by a combination of sol-gel auto combustion and ultrasonic irradiation techniques

S. Abedini Khorrami[a,*], G. Mahmoudzadeh[a], S. S. Madani[a] and F. Gharib[b]
[a]*Chemistry Department, North Tehran Branch, Azad University, Tehran, Iran*
[b]*Chemistry Department, Shahid Beheshti University, Tehran, Iran*

$ZnFe_2O_4$ nanocrystallites were synthesized successfully by a combination of sol-gel auto combustion and ultrasonic irradiation techniques. The influence of the calcination temperature on the particle sizes was investigated. The particles have been calcined at temperatures varying from 400 to 900 °C. The studies were carried out using XRD and SEM techniques. The gradual increase in the crystallite size with the calcination temperature indicates the formation of bigger particles by the calcination.

Key words: $ZnFe_2O_4$, Sol-gel, Auto-combustion, Ultrasonic, SEM, XRD.

Introduction

Ferrite magnetic materials are among the most important materials used today in modern technology. Spinels of the type $A^{2+}B^{3+}{}_2O_4$ have attracted considerable attention due to their wide applications in several technological fields [1], where A and B refer to the tetrahedral and octahedral sites respectively in the oxygen lattice. $ZnFe_2O_4$ is one of the most important spinel ferrites which have attractive properties for application as soft magnets and low loss materials at high frequencies [2]. As is well known, the stoichiometric composition is $ZnFe_2O_4$ and possesses a normal spinel structure, is a commercially important material because of its excellent electrical and magnetic properties [3]. They are used as an important part in many applications as in wave applications, radio electronics and sensors [4]. The physical properties of ferrites are dependent on several factors such as the preparation method, sintering process, and the type and amount of constituent elements or additives [5]. There are two main factors which make nanomaterials to behave significantly differently than that of bulk materials: (I) surface effects (causing a smooth scaling of properties due to the fraction of atoms on the surface) and (II) quantum effects (showing discontinuous behavior due to quantum confinement effects in materials with delocalized electrons) [6]. These factors affect the chemical reactivity of materials and physical properties such as; mechanical, optical, electrical and magnetic properties. $ZnFe_2O_4$, one of the iron-based cubic spinel series, shows striking changes in its magnetic properties by reducing the grain size to the nanometre-sized range. Bulk zinc ferrite is a completely normal spinel structure with Zn ions in the tetrahedral or A sites and Fe ions in the octahedral or B sites [7]. Various synthesis methods, such as dry and wet-milling [8], sol-gel, co-precipitation [9], microemulsion [10], pulsed laser deposition, electrode position [11], thermal solid-state reaction [12] and an ultrasonic cavitation approach [13] have been reported to prepare nanometre $ZnFe_2O_4$ particles.

The sol-gel method, in particular, is one of the most useful and attractive techniques for the synthesis of nanosized ferrite materials because of its advantages such as; good stoichiometric control and the production of ultrafine particles with a narrow size distribution in a relatively short processing time at a very low temperature [14]. It is a novel method with a combination of a chemical sol-gel process and a combustion process. This method uses a solution during the initial step of the preparation process, which leads to the following advantages: (1) reactants are well-dispersed, providing a homogeneous reaction mixture; (2) reactants are in a much higher reactive state than in the corresponding solid-state reaction precursors; (3) consequently, the reaction requires less energy, and the initial reaction threshold temperature can be lowered; and (4) distribution of the components in mixed solids is more uniform and random because of the homogeneous starting mixture [15]. It is for these reasons that the sol-gel auto combustion method is widely applied for preparing ceramic and magnetic materials [14].

Recently, research into combustion synthesis of ferrites has been given much attention due to the high productivity, low consumption of energy, and simplicity of the process. The size of the particles can be varied by changing the solution composition, pH, and calcination temperature [16]. It has been observed that the calcination temperature is an important parameter during the synthesis of zinc ferrite via a sol-gel method which affects the physical properties of zinc ferrite nanoparticles. It has been observed that the $ZnFe_2O_4$ synthesized at different temperatures exhibit different particle sizes and thus show different

*Corresponding author:
Tel :+98-912-4403059
Fax: +98-21-22222512
E-mail: S_akhorrami@iau-tnb.ac.ir

magnetic properties such as saturation magnetization, coercivity, and remanent magnetization.

Ultrasonic cavitation chemistry, an approach for synthesizing in variety of compounds in milder conditions is already the rage in materials technology. Over the last few years, this technique has also started to catch on in the materials science community as a way to speed discoveries in this area. The major advantage of this new method is that it affords a reliable and easy route for the control of both the synthetic process and nanostructure in advanced materials [17].

Experimental

Zinc nitrate tetra hydrate (Zn $(NO_3)_2 \cdot 4H_2O$, Merck), iron nitrate nona hydrate (Fe $(NO_3)_3 \cdot 9H_2O$, Merck), glycine ($C_2H_5NO_2$, Merck) and NH_4OH (Merck, 25%) was obtained of analytical grade. All materials were used without further purification. All experimental studies were done with deionized water. $ZnFe_2O_4$ powders were synthesized by a combination of sol-gel auto combustion and ultrasonic irradiation techniques (HF-Frequenz 35 kHz, 240 W/ Made in Germany). The phase identification of the burnt powder of $ZnFe_2O_4$ was done using XRD (Model: XPERT- MPD, Philips operated at 40 kV and 40 mA). The structural morphology was investigated using SEM (Phillips XL30 with 40 kV operating voltage).

Zinc ferrite preparation

The preparation process is described as follows: the molar ratio of Zn to Fe ions was 1 : 1. First certain amounts of glycine were weighed and dissolved in a minimum of deionzed water, then Zn and Fe ions were dissolved with a molar ratio of total nitrates to glycine (1 : 2). A small amount of ammonia was added into the solution to adjust the pH value to about 7 which stabilized the sol. During this procedure, the solution was continuously stirred for 6 h and kept at a temperature of 60 ºC. When temperatures higher than 350 ºC were necessary to induce the auto-combustion, a Teflon vessel was put directly on the hotplate at 350 ºC. The sol turned into a gel with a high viscosity and the color changed as brown. The dried gel simultaneously burnt in a self-propagating combustion manner until it was completely transformed into loose powder. The spontaneous combustion lasted for about 10-20 seconds, until the gel was completely burnt out to form a loose powder. Finally the as-burnt powder was calcined at 500 ºC for 3 h. Then, the product was placed in an ultrasonic irradiation bath at 25 ºC for 15 minutes.

Results and Discussion

The dried gels, formed from metal nitrates and glycine with a molar ratio of 1 : 1.2, exhibit self-propagating combustion behavior. When the dried gel was ignited at any point in the air, the combustion rapidly propagated forward until all the gel was completely burnt out to form loose powders. The overall process involves three steps: formation of a homogeneous sol; formation of a dried gel; and combustion of the dried gel.

When ultrasound is introduced into this method, the nucleation rate is further increased, vast amounts of micro air bubbles are formed due to ultrasonic cavitate. These micro air bubbles can disturb the ordered crystal sequence. They will affect the crystals growing further. A shock wave with a high pressure and a micro-emission fluid produced by ultrasonic cavitation can bring comminution and emulsification, stirring, and others mechanical influences. It can effectively prevent the crystal growth and aggregation. Small size nanoparticles with a uniform size distribution are easily obtained. The ultrasound has a small effect on the crystal growth rate. But the mechanical influence produced by ultrasonic cavitation can prevent the crystals growing.

The mechanical influence produced by ultrasonic cavitation such as comminution, emulsification, stirring, and others, can prevent the crystal growth and aggregation. But when the ultrasonic time was too long, a shock wave with a high pressure, a micro-emission fluid and "the Brownian phenomenon" of a nanoparticle itself could make nanoparticles aggregated. A longer ultrasonic time leads to more serious aggregation. The optimal ultrasonic time was about 20 minutes [18]. On the other hand, the results have shown that with an increase in the calcination temperature, the intensity of peaks increases and the diffraction peaks become sharper and narrower. This indicates an enhancement of the crystallites which originated from an increment of the crystallite volume ratio due to a size enlargement of the nuclei.

The XRD patterns of the zinc-ferrite samples calcined at different temperatures varying from 400 to 900 ºC are shown in Fig. 1. Also, the SEM images of Zn-ferrite samples calcined at 400-900 ºC are given in Fig. 2.

The influence of the calcination temperature on the crystallite sizes of the Zn-ferrite samples is shown in Fig. 3 and Table 1. The crystallite size for all samples prepared at different calcination temperatures was estimated from XRD peak broadening using Scherrer's equation:

$$D = \frac{0.9\lambda}{\beta \cos\theta} \quad (1)$$

where D is the crystallite size, λ is the wavelength of X-ray radiation (Cu Kα), θ is the Bragg angle and β is the full width at half maximum (FWHM) of the most intense diffraction peak (2 2 7). Decomposition temperatures are different for different intermediates. Decomposition temperature of the same intermediates is related to the precursors [19].

When the calcination temperature is low, the intermediate might not be decomposed completely. The calcinations time must be prolonged to make the intermediate decompose. Different size crystals have different vapor pressures. The vapor pressure of a small size crystal is high and the vapor pressure of a large size crystal is low. So the process that a small size crystal turns into a big size crystal will

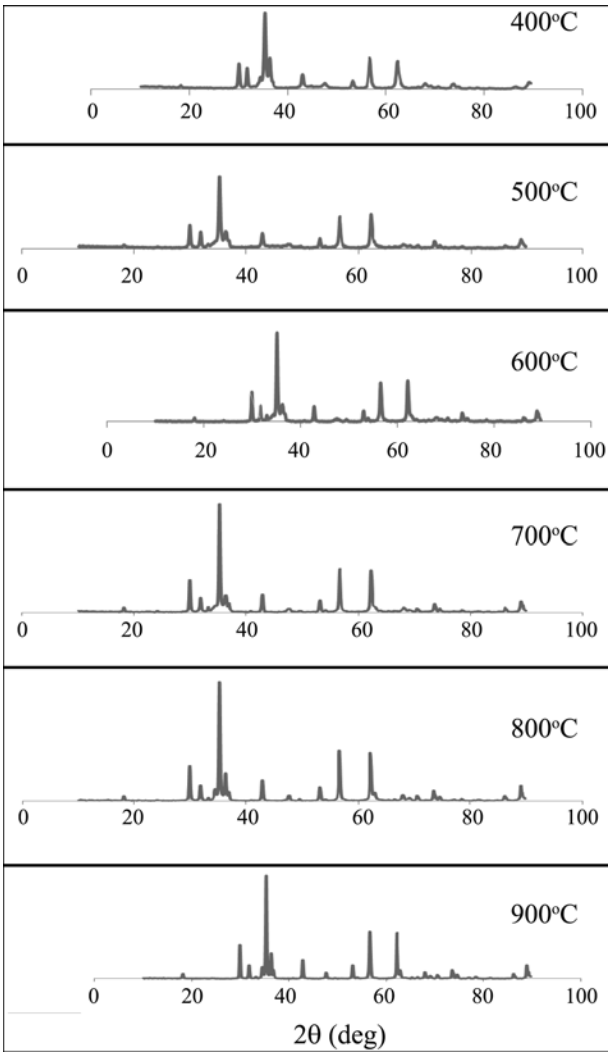

Fig. 1. XRD patterns of the zinc-ferrite samples calcined at different temperatures from 400 to 900 °C.

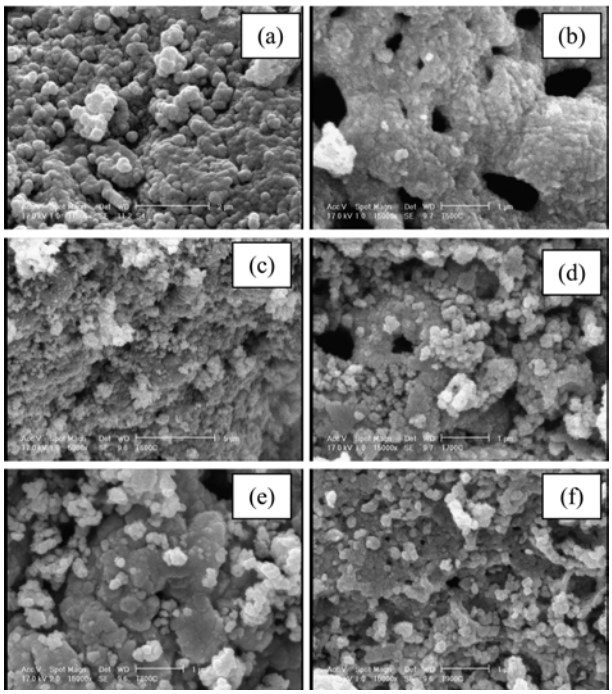

Fig. 2. SEM images of (a) powder precursor and Zn- ferrites calcined at (a) 400, (b) 500, (c) 600, (d) 700, (e) 800 and (f) 900 °C.

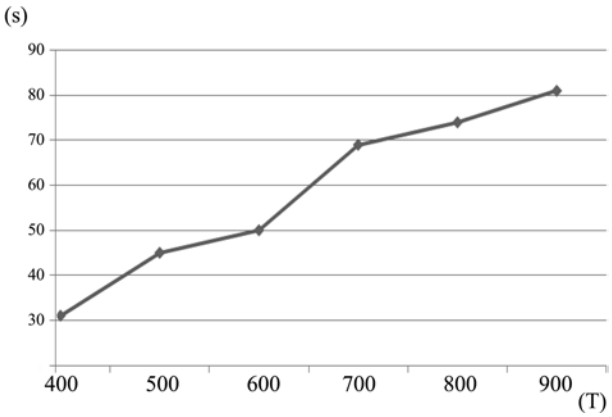

Fig. 3. Dependence of the crystallite sizes of Zn-ferrites calcined at different temperatures.

Table 1. The dependence of average size of Zn- ferrite (franklinite) on calcination temperature

Calcination temperature (°C)	Average size franklinite (nm)
400	31
500	45
600	50
700	69
800	74
900	81

happen automatically.

This process (a small size crystal disappears and a large size crystal grows bigger than before) proceeds very quickly, especially at a high temperature. When the calcination time is prolonged, the process will be achieved completely. For a crystal that exists for a long time at a high calcination temperature; the crystal size will easily become bigger. Thus, nano-particles with a large size and a wide size distribution can be produced. For the same reason, although the intermediate can be completely decomposed quickly at a high calcination temperature, nano-particles with a large size are easily obtained due to aggregation. So, in order to get nano-particles having a small size and high surface area, the calcination temperature should not be high and the calcination time should not be too long [18].

All of the diffraction peaks (in Fig. 1) confirmed the formation of the pure phases zinc ferrite with a face centred cubic spinel and *Fd*3*m* (2 2 7) space group, zincite with a hexagonal and $p6_3$ mc (1 8 6) space group and hematite with a rhombohedral and R3c (1 6 7) space group. No diffraction peaks of other impurities were observed in the patterns.

An X-ray diffraction system was used to check the structure of the samples prepared. Cu-Kα radiation with λ = 1.54 Å was used. The diffraction patterns were collected

and from the peak positions, each corresponding to a set of (h, k and l) planes. The d spacing between planes was estimated using Bragg's law:

$$n\lambda = 2\ d\ sin\theta \tag{2}$$

The lattice parameter "a" for the cubic ferrite structure can be estimated using the relation:

$$\frac{1}{d^2} = \frac{k^2+h^2+1^2}{a^2} \tag{3}$$

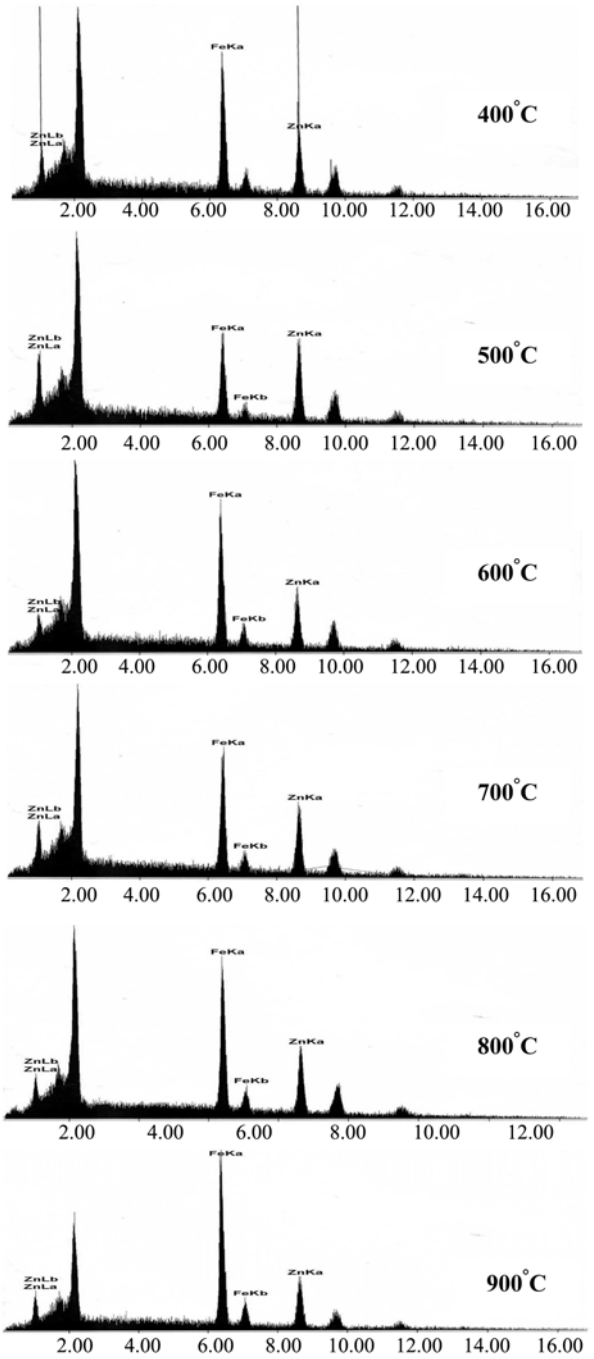

Fig. 4. EDAX analysis of the Zn-ferrite samples calcined in different temperatures (400- 900 °C).

The X-ray density for all samples prepared was calculated using:

$$D_x = \frac{8M}{N_A \times a^2} \tag{4}$$

where M is the molar mass of the ferrite, and N_A is Avogadro's number. The lattice parameter and X-ray density (D_x) for the cubic ferrite structure was calculated as 8.44107 (Å) and 5.33 (g/cm^3), respectively.

The composition of the samples has been determined using energy dispersion X-ray analysis (EDAX) and the patterns obtained at different temperatures (400-900 °C) are shown in Fig. 4. The EDAX spectra revealed the presence of ZnO and Fe_2O_3 peaks in the samples which is in agreement with XRD results as it clearly shows that the precursor materials have been completely removed from the product. From the EDAX results it is considered that all the nanocrystallites are pure and in Table 3 the compositions are given.

The SEM images of the Zn-ferrite samples (Fig. 2) show that the morphology of particles were almost spherical, regular in shape and dispersed uniformly, but agglomerated to some extent due to the interaction between the magnetic nanoparticles, whereas the gel exhibits a relatively porous network. The pressure exercised by gaseous species should be responsible for the breakup of the porous structure. Heat treatment resulted in agglomeration of the powder as a function of the calcining temperature which is typical for the spinel ferrites. Therefore, some degree of agglomeration at the higher calcination temperature appears

Table 2. The dependence of average sizes of phases to the calcination temperature

	Average sizes (nm)	
Calcination temperature (°C)	Fe_2O_3	ZnO
400	-	37
500	27	33
600	49	54
700	71	30
800	55	34
900	57	23

Table 3. EDAX Quantification (standard less) oxides

Oxides	Wt %	Calcination temperatures (°C)
Fe_2O_3 ZnO	45.88	400
	54.12	
	28.12	500
	71.88	
	41.33	600
	58.62	
	48.09	700
	51.91	
	45.52	800
	54.48	
	56.29	900
	43.71	

unavoidable. In many cases of nanocrystalline ferrites, it is observed that there is a tendency of agglomeration among the nanoparticles [14].

Conclusions

Nanocrystalline $ZnFe_2O_4$ powders were successfully synthesized by a combination of the sol-gel auto combustion and ultrasonic irradiation methods. Results show that with an increase in the calcination temperature, the intensity of peaks increases and the diffraction peaks become sharper and narrower. The observed particle size increases with the calcination temperature and reachs to 81 nm at 900 oC. It seems that two or more particles fuse together by melting of their surfaces through the calcination process. Therefore, a gradual increase in the crystallite size with the calcination temperature indicates the formation of bigger particles with the temperature calcination. This is attributed to the grain growth of the particles in the nanoregion at a temperature well below the melting temperature of bulk ferrites.

References

1. J.S. Bettinger, R.V. Chopdekar, M. Liberati, J.R. Neulinger, M. Zhshiev and Y. Akamwa, J. Magn. Magn. Mater. 318[1-2] (2007) 65-73.
2. S. Son, M. Taheri, E. Carpenter, V.G. Harris and M.E. McHenry, J. Appl. Phys. 91[10] (2002) 7589-7591.
3. S. Bera, A.A.M. Prince and S. Velmurugan, J. Mater. Sci. 36[22] (2001) 5379-5384.
4. N. Rezlescu, E. Rezlescue, C. Sava, F. Tudorache and P. Popa, Turk. J. Phys., 28[6] (2004) 391-396.
5. P. Yadoji, R. Peelamedu, D. Agrawal and R. Roy, Mater. Sci. Eng. B 98[3] (2003) 269-278.
6. E. Roduner, Chem. Soc. Rev. 35[7] (2006) 583-592.
7. Y. Changwa, Z. Qiaoshi, G.F. Goya, T. Torres, L. Jinfang, W. Haiping, G. Mingyuan, Z. Yuewu, W. Youwen and J.Z. Jiang, J. Phys. Chem. C, 111[33] (2007) 12274-12278.
8. S. Ozcan, B. Kaynar, M.M. Can and T. Firat, Mater. Sci. Eng. B, 121[3] (2005), 278-281.
9. M. Atif, S.K. Hasanain and M. Nadeem, Solid State Commun. 138[8] (2006) 416-421.
10. P. Komar, "In Handbook of Microemulsion Science and Technology", Ed., Dekker, (New York, 1999).
11. N. Wakiya, K. Muraoka, T. Kiguchi, N. Mizutani and K. Shinozaki, J. Magn. Magn. Mater. 310[2] (2007) 2546-2548.
12. F.S. Li, H.B. Wang, L. Wang and J.B. Wang, J. Magn. Magn. Mater. 309[2] (2006) 295-299.
13. M. Sivakumar, A. Towata, K. Yasui, T. Tuziuti and Y. Iida, Curr. Appl. Phys. 6[3] (2006) 591-593.
14. M. Srivastava, S. Chaubey and K.O. Animesh, Mater. Chem. Phy.118[1] (2009) 174-180.
15. C.J. Brinker and G.W. Scherer, "Sol-Gel Science. The Physics and Chemistry of Sol-Gel Processing", Academic Press, (San Diego, 1990).
16. L. Satyanarayana, K. Madhusudan Reddy and S.V. Manorama, Mater. Chem. Phys. 82[1] (2003) 21-26.
17. L.E. Tavakoli, M. Sohrabi and A. Kargari, Chem. Pap. 61[3] (2007) 151-170.
18. Z.X. Tang and L.E Shi, Ecl. Quim. 33 (2008)15-20.
19. W. Shan, X. Zheng and C. Jinxin, Acta Scientiarum Naturalium Universitatis Nankaiensis, 37[1] (2004) 73-74.